



Complexes containing benzimidazolyl-phenol ligands and Ln(III) ions: Synthesis, spectroscopic studies and preliminary cytotoxicity evaluation

Andrea Hernández-Morales^a, José María Rivera^a, Aracely López-Montea^a, Soledad Lagunes-Castro^a, Silvia Castillo-Blum^b, Karla Cureño-Hernández^b, Angelina Flores-Parra^c, Osvaldo Villaseñor-Granados^c, Raúl Colorado-Peralta^{a,*}

^a Maestría en Ciencias en Procesos Biológicos, FCQ-UV, C.P. 94340 Orizaba, Ver., Mexico

^b Departamento de Química Inorgánica, FQ-UNAM, C.P. 04510 CDMX, Mexico

^c Departamento de Química, CINVESTAV-IPN, C.P. 07360 CDMX, Mexico

ARTICLE INFO

Keywords:

Cytotoxicity
Lanthanides
Benzimidazoles
Bidentate ligands
DFT calculations
HeLa cells

ABSTRACT

Fourteen new complexes were obtained from Ln(III)(NO₃)₃·n-H₂O and the chromophores 2-(1H-benzo[d]imidazol-2-yl)-phenol (**Bzp1**) or 2-(5-methyl-1H-benzo[d]imidazol-2-yl)-phenol (**Bzp2**). The complete characterization allowed us to assign unequivocally the structures of all the complexes. The techniques used for this purpose were Ultraviolet-Visible (UV-Vis) and Fourier-Transform Infrared (FT-IR) spectroscopies, High-Resolution Mass Spectrometry (HRMS), Magnetic Susceptibility (MS), Elemental Analysis (EA) and Molar Conductivity (MC). HRMS allowed us to find the molecular ion and its isotopic pattern. The FT-IR spectral data suggested that benzimidazolyl-phenol ligands coordinate with Ln(III) ions through iminic nitrogen and phenolic oxygen. Thermogravimetric Analysis (TGA) studies of **NdBzp1** and **GdBzp2** complexes indicate the presence of lattice water along with three nitrates and two benzimidazolyl-phenol ligands; the thermal decomposition was consistent with the minimal formula suggested by EA. The coordination type of the benzimidazolyl-phenol ligands, the geometry and the structural organization of these coordination complexes have been interpreted by Density Functional Theory (DFT) calculations, and they coincided with the physicochemical data suggesting a coordination number eight for the Ln(III) ions. The cytotoxicity of the chromophores and their coordination complexes was tested against a cancer cell line (HeLa), as compared with structure/support cells (NIH-3T3) and defense cells (J774A.1), revealing that three coordination complexes showed moderate cytotoxicity against the cell lines studied.

1. Introduction

Benzimidazole derivatives have an extensive diversity of pharmacological and biological applications due to their structural relationship with purines and pyrimidines [1,2]. In addition, vitamin B₁₂ contains a 5,6-dimethyl-benzimidazole fragment coordinated to the Co(III) ion [3,4]. Literature data describe a large amount of properties for benzimidazole derivatives, such as antiparasitic, antioxidant, anti-inflammatory, analgesic, antihypertensive, anthelmintic, antiprotozoal, anticancer, antimicrobial, among others [5]. In addition, they are active constituents of biocides, such as fungicides and insecticides, and they have formed important compounds in photochemical, photophysical and bioinorganic chemistry [6]. Benzimidazole derivatives are ligands extensively used in coordination chemistry, due to their structural stability and low reactivity [7]; therefore, there is a great interest in

synthesizing and characterizing metal complexes of the *p*, *d* and *f* block with benzimidazolic ligands [8,9].

Additionally, the benzimidazolyl-phenol derivatives act as a bidentate (N,O) ligand [10–12]. The complexes with these ligands are important, due to their thermal stability, optical properties, catalytic efficiency and their biological applications [13–26]. The benzimidazolyl-phenol complexes are a novel category of photochemical compounds that can be handled as electroluminescent materials, whose properties can be delimited using diverse metal ions [27–29]. In this sense, metal complexes are of unlimited importance for OLED technology, as specified by numerous patents [30]. The benzimidazolyl-phenol complexes are also useful as high-energy radiation detectors, laser dyes, molecular energy storage systems, fluorescent probes and selective complexes for determining Hg(II) [31–36]. The deprotonated species of these organic ligands are appropriate for the creation of

* Corresponding author.

E-mail address: racolorado@uv.mx (R. Colorado-Peralta).

<https://doi.org/10.1016/j.jinorgbio.2019.110842>

Received 30 April 2019; Received in revised form 6 September 2019; Accepted 7 September 2019

Available online 11 September 2019

0162-0134/ © 2019 Elsevier Inc. All rights reserved.

different metal complexes with diverse coordination modes, structural arrangement and geometry [37–45]. The oxygen atoms of the deprotonated hydroxyl group generally act as a terminal ligand or a bridge ligand, although there are reports in which the proton is not lost by coordinating different transition metals [46–50].

On the other hand, the coordination chemistry of the Ln(III) ions is growing speedily, due to the importance of these complexes in basic and applied research in different technological and scientific fields, such as the natural sciences, engineering, medical and health sciences [51–55]. Ln(III) complexes have attracted attention to the field of bioinorganic chemistry, since some of their compounds are being used in biomedical assays as MRI contrast agents [56,57]. They can be employed as biological probes in clinical chemistry and molecular biology due to their exceptional biological and photophysical properties [58,59]. The Ln(III) complexes have motivated countless attempts in the design of potential anticancer agents, due to their electronic configuration $[\text{Xe}]4f^{1-14}5d^{0-1}6s^2$ and its analogy with Ca(II). The Ln(III) ions have ionic radii similar to that of Ca(II) ions, but due to their larger charge, they show a high affinity for the sites that Ca(II) occupies in biological systems and generate strong bonds with the water molecules [61–66]. The Ca(II)-dependent enzymes can be inhibited by the Ln(III) ions, but in some cases they have also been activated by them. Thus, the inhibitory or activating effect of the Ln(III) ions could be related to the particular function of the Ca(II) ions in the native enzymes [67,68].

The Ln(III) ions have diverse biological effects, it has been demonstrated that in some cases they promote cell proliferation and in others, they induce apoptosis. Therefore, there are some reports with compounds that have shown a cytotoxic effect when studying several cancer cell lines [69–73]. Among other effects, it has been shown that Ln(III) ions can induce cell membrane perforation and apoptosis, they also seem to have some influence in the control of oxidative damage produced by free radicals and other reactive oxygen species, these being the main mechanisms of anti-cancer activity. Some authors emphasize that Ln(III) complexes have the ability to interact directly with DNA, preventing their relaxation through the inhibition of topoisomerases [74,75].

Finally, the Ln(III) complexes coordinated to benzimidazolyl-phenol ligands are an area of interest, because they reveal ligand-to-metal charge transfer processes (LMCT), as well as a supramolecular disposition built on hydrogen interactions and π - π stacking [76–80]. However, there are no studies describing the cytotoxic activity of this class of benzimidazolyl complexes with Ln(III) ions; therefore, we have synthesized Ln(III) complexes with benzimidazolyl-phenol ligands and we discuss their selective cytotoxicity between cancer cells, structure/support cells and defense cells.

2. Experimental

2.1. Materials and instrumentation

In this project, reagents and solvents purchased from Sigma-Aldrich Chemical Co. were employed. The solvents used were purified according to the literature [81]. Melting points were determined in a Thermo Scientific Electrothermal (model IA9100) instrument in sealed capillaries. Elemental analyses were quantified in the analyzers: Flash Thermo Finnigan (model 1112) and Perkin Elmer (model 2400). NMR spectra of the samples in DMSO- d_6 solutions were acquired in the spectrometers: Bruker Avance 300 (^{13}C : 75.47 MHz and ^1H : 300.13 MHz) and Jeol GSX-Delta 270 (^{13}C : 67.94 MHz and ^1H : 270.17 MHz) with 5 mm diameter tubes. Chemical shifts expressed in ppm were corrected using tetramethylsilane as reference; coupling constants were informed in Hertz. IR spectra (400 – 4000 cm^{-1}) of the solid samples were acquired on a FT-IR Perkin Elmer (model Spectrum 100) spectrometer with a universal ATR polarization accessory. High resolution mass data were recorded in an Agilent Technologies LC/MSD-TOF (model 6210, G1969A) spectrometer coupled to HPLC, with

electrospray (ES) as ionization source and acetonitrile as solvent.

Electronic absorption spectra (200–1200 nm) of solid samples were recorded on a Varian Cary (model 6000i) spectrometer by diffuse reflectance. Emission and excitation spectra (290–950 nm) of solid samples were acquired in a Horiba Scientific (model FluoroMax-4p) equipment, with a 150 W continuous emission xenon lamp. Effective magnetic moments of the solid samples were determined on a Johnson Mathey (model MKII) balance by the Gouy method. Thermograms were obtained in a Perkin Elmer (model TGA 4000) thermogravimetric analyzer with a heating rate of $10^\circ\text{C}/\text{min}$, under controlled nitrogen atmosphere and temperature range of 25–500 $^\circ\text{C}$. Molar electrical conductivity was determined from methanol $1 \times 10^{-3}\text{ M}$ solutions using an ORION (model 140) conductivity meter.

2.2. Synthesis

2.2.1. Preparation of 2-(1H-benzo[d]imidazol-2-yl)-phenol (Bzp1)

The procedure reported by Quezada-Buendía et al., in 2008 was utilized with some modifications that are mentioned below [22]. In a round flask with magnetic stirring were placed: 1 g of 1,2-diaminobenzene (9.2472 mmol), 1.2772 g of 2-hydroxybenzoic acid (9.2472 mmol) and 10 g of polyphosphoric acid, which were heated for 6 h at a temperature of 220 $^\circ\text{C}$. The reaction mixture was slowly cooled to room temperature, and then 100 mL of distilled water was added and neutralized by the addition of reagent grade ammonium hydroxide dropwise. A gray precipitate was separated from the reaction mixture, which was filtered and dissolved in 100 mL of methyl alcohol. A yellow product crystallized slowly from the solution and was obtained with a yield of 93% (1.8079 g, Mp 268 $^\circ\text{C}$). NMR (δ ppm, DMSO- d_6 , 25 $^\circ\text{C}$) ^1H : 8.80 (sa, 1H, OH), 8.12 (d, 1H, H-9, 3J 7.9 Hz), 7.67 (d, 2H, H-4, H-7, 3J 6.0 Hz), 7.37 (dd, 1H, H-11, 3J 7.5, 8.9 Hz), 7.25 (dd, 2H, H-5, H-6, 3J 6.0 Hz), 7.04 (d, 1H, H-12, 3J 7.5 Hz), 7.00 (dd, 1H, H-10, 3J 7.9, 8.9 Hz). ^{13}C : 158.0 (C-13), 151.9 (C-2), 137.2 (sa, C-3a, C-7a), 132.5 (C-11), 126.9 (C-9), 123.6 (C-5, C-6), 120.1 (C-10), 117.7 (C-12), 115.3 (C-4, C-7), 113.1 (C-8). FT-IR (ATR, $\nu\text{ cm}^{-1}$): 3324.9 (N–H), 3100.0 (O–H), 1603.3, 1562.4, 1489.8, 1461.8 (C=C) $_{\text{arom}}$, 1603.3 (C=N), 1262.2 (C–N), 1077.9 (C–O), 749.6 (C–H) $_{\text{arom}}$. (+)TOF m/z (amu): Calc. for $(\text{C}_{13}\text{H}_{11}\text{N}_2\text{O})^+$: 211.0871. Found: 211.0866. Anal. Calc. for $\text{C}_{13}\text{H}_{10}\text{N}_2\text{O}$: C, 74.3; H, 4.8; N, 13.3. Found: C, 74.2; H, 4.8; N, 12.9.

2.2.2. Preparation of 2-(5-methyl-1H-benzo[d]imidazol-2-yl)-phenol (Bzp2)

In a round flask with magnetic stirring were placed: 1 g of 3,4-diaminotoluene (8.1853 mmol), 1.1306 g of 2-hydroxybenzoic acid (8.1853 mmol) and 10 g of polyphosphoric acid, which were heated for 6 h at a temperature of 220 $^\circ\text{C}$. The reaction mixture was slowly cooled to room temperature, and then 100 mL of distilled water was added and neutralized by the addition of reagent grade ammonium hydroxide dropwise. A gray precipitate was separated from the reaction mixture, which was filtered and dissolved in 100 mL of methyl alcohol. A pink product crystallized slowly from the solution and was obtained with a yield of 72% (1.3217 g, Mp 310 $^\circ\text{C}$). NMR (δ ppm, DMSO- d_6 , 25 $^\circ\text{C}$) ^1H : 8.71 (sa, 1H, OH), 8.03 (d, 1H, H-9, 3J 7.9 Hz), 7.54 (s, 1H, H-4), 7.44 (d, 1H, H-7, 3J 7.5 Hz), 7.36 (dd, 1H, H-11, 3J 7.0, 7.9 Hz), 7.09 (d, 1H, H-6, 3J 7.5 Hz), 7.02 (d, 1H, H-12, 3J 7.0 Hz), 7.00 (dd, 1H, H-10, 3J 7.9, 7.9 Hz), 2.25 (s, 3H, H-14). ^{13}C : 158.4 (C-13), 151.9 (C-2), 137.0 (sa, C-3a, C-7a), 132.8 (C-5), 132.1 (C-11), 126.6 (C-9), 124.6 (C-6), 119.6 (C-10), 117.6 (C-12), 115.3 (C-4, C-7), 113.2 (C-8), 21.7 (C-14). FT-IR (ATR, $\nu\text{ cm}^{-1}$): 3211.9 (N–H), 3100.0 (O–H), 1625.4, 1561.5, 1486.9, 1457.0 (C=C) $_{\text{arom}}$, 1623.8 (C=N), 1257.8 (C–N), 1070.8 (C–O), 722.3 (C–H) $_{\text{arom}}$. (+)TOF m/z (amu): Calc. for $(\text{C}_{14}\text{H}_{13}\text{N}_2\text{O})^+$: 225.1027. Found: 225.1022. Anal. Calc. for $\text{C}_{14}\text{H}_{12}\text{N}_2\text{O}$: C, 75.0; H, 5.4; N, 12.5. Found: C, 74.9; H, 5.4; N, 12.9.

2.2.3. General method for the preparation of the lanthanide(III) complexes

A solution with one equivalent of Ln(III)(NO₃)₃ \cdot n -H₂O (Ln(III) = La,

Nd, Sm, Eu, Gd, Tb, Dy) in 20 mL of methyl alcohol was prepared and it was named solution **A**. Another solution was prepared with two equivalents of the ligand (**Bzp1** or **Bzp2**) in 20 mL of methyl alcohol and it was named solution **B**. Solution **A** was slowly added dropwise to solution **B**, in a round flask with magnetic stirring, subsequently it was refluxed for 2 h. The reaction mixture was filtered and evaporated using vacuum.

2.2.3.1. [La(III)(Bzp1)₂(NO₃)₂]NO₃·5 H₂O (LaBzp1**).** The compound **LaBzp1** was synthesized following the procedure described in Section 2.2.3. from 102.97 mg of La(III)(NO₃)₃·6 H₂O (0.2378 mmol) and 100 mg of **Bzp1** (0.4757 mmol). A yellow product was obtained with a yield of 83.0% (0.1684 g, Mp 225 °C). FT-IR (ATR, ν cm⁻¹): 3064.9 (N–H), 3200.0 (O–H), 1624.3, 1609.9, 1561.7, 1498.3 (C=C)_{arom}, 1624.3 (C=N), 1289.4 (C–N), 1241.2 (C–O), 750.6 (C–H)_{arom}; NO₃ bands: 1458.4 (ν_1), 1393.4 (ν_0), 1289.5 (ν_4), 1022.5 (ν_2), 840.0 (ν_6), 815.3 (ν_3), 798.7 (ν_5). (+)TOF *m/z* (amu): Calc. for (C₂₆H₂₀N₆O₈La)⁺: 683.0403. Found: 683.0407. Anal. Calc. for C₂₆H₃₀LaN₇O₁₆: C, 37.4; H, 3.6; N, 11.7. Found: C, 37.7; H, 3.5; N, 11.9.

2.2.3.2. [Nd(III)(Bzp1)₂(NO₃)₂]NO₃·3 H₂O (NdBzp1**).** The compound **NdBzp1** was synthesized following the procedure described in Section 2.2.3. from 104.24 mg of Nd(III)(NO₃)₃·6 H₂O (0.2378 mmol) and 100 mg of **Bzp1** (0.4757 mmol). A yellow product was obtained with a yield of 89.6% (0.1714 g, Mp 288 °C). FT-IR (ATR, ν cm⁻¹): 3065.4 (N–H), 3236.3 (O–H), 1624.9, 1609.9, 1562.5, 1499.1 (C=C)_{arom}, 1624.9 (C=N), 1289.2 (C–N), 1241.1 (C–O), 751.1 (C–H)_{arom}; NO₃ bands: 1457.1 (ν_1), 1393.8 (ν_0), 1289.3 (ν_4), 1022.3 (ν_2), 839.7 (ν_6), 815.2 (ν_3), 799.1 (ν_5). (+)TOF *m/z* (amu): Calc. for (C₂₆H₂₀N₆O₈Nd)⁺: 686.0420. Found: 686.0417. Anal. Calc. for C₂₆H₂₆NdN₇O₁₄: C, 38.8; H, 3.3; N, 12.2. Found: C, 39.1; H, 3.0; N, 12.3.

2.2.3.3. [Sm(III)(Bzp1)₂(NO₃)₂]NO₃·3 H₂O (SmBzp1**).** The compound **SmBzp1** was synthesized following the procedure described in Section 2.2.3. from 105.69 mg of Sm(III)(NO₃)₃·6 H₂O (0.2378 mmol) and 100 mg of **Bzp1** (0.4757 mmol). A yellow product was obtained with a yield of 90.5% (0.1746 g, Mp 192 °C). FT-IR (ATR, ν cm⁻¹): 3065.2 (N–H), 3200.0 (O–H), 1624.4, 1610.1, 1499.0, 1479.6 (C=C)_{arom}, 1624.4 (C=N), 1290.1 (C–N), 1241.8 (C–O), 750.7 (C–H)_{arom}; NO₃ bands: 1459.8 (ν_1), 1392.6 (ν_0), 1290.1 (ν_4), 1022.3 (ν_2), 839.2 (ν_6), 818.9 (ν_3), 798.6 (ν_5). (+)TOF *m/z* (amu): Calc. for (C₂₆H₂₀N₆O₈Sm)⁺: 688.0463. Found: 688.0469. Anal. Calc. for C₂₆H₂₆SmN₇O₁₄: C, 38.5; H, 3.2; N, 12.1. Found: C, 38.6; H, 3.3; N, 12.4.

2.2.3.4. [Eu(III)(Bzp1)₂(NO₃)₂]NO₃·4 H₂O (EuBzp1**).** The compound **EuBzp1** was synthesized following the procedure described in Section 2.2.3. from 101.79 mg of Eu(III)(NO₃)₃·5 H₂O (0.2378 mmol) and 100 mg of **Bzp1** (0.4757 mmol). A yellow product was obtained with a yield of 86.8% (0.1714 g, Mp 297 °C). FT-IR (ATR, ν cm⁻¹): 2942.8 (N–H), 3200.0 (O–H), 1624.4, 1609.8, 1562.1, 1458.7 (C=C)_{arom}, 1624.4 (C=N), 1289.6 (C–N), 1241.2 (C–O), 751.0 (C–H)_{arom}; NO₃ bands: 1458.7 (ν_1), 1392.8 (ν_0), 1289.7 (ν_4), 1022.2 (ν_2), 835.0 (ν_6), 817.6 (ν_3), 798.2 (ν_5). (+)TOF *m/z* (amu): Calc. for (C₂₆H₂₀N₆O₈Eu)⁺: 697.0555. Found: 697.0549. Anal. Calc. for C₂₆H₂₈EuN₇O₁₅: C, 37.6; H, 3.4; N, 11.8. Found: C, 37.2; H, 3.8; N, 11.9.

2.2.3.5. [Gd(III)(Bzp1)₂(NO₃)₂]NO₃·4 H₂O (GdBzp1**).** The compound **GdBzp1** was synthesized following the procedure described in Section 2.2.3. from 107.33 mg of Gd(III)(NO₃)₃·6 H₂O (0.2378 mmol) and 100 mg of **Bzp1** (0.4757 mmol). A yellow product was obtained with a yield of 87.7% (0.1744 g, Mp 270 °C). FT-IR (ATR, ν cm⁻¹): 3152.9 (N–H), 3200.0 (O–H), 1610.6, 1602.4, 1596.1, 1561.4 (C=C)_{arom}, 1602.4 (C=N), 1289.0 (C–N), 1259.2 (C–O), 737.6 (C–H)_{arom}; NO₃ bands: 1462.5 (ν_1), 1401.3 (ν_0), 1304.9 (ν_4), 1022.0 (ν_2), 839.9 (ν_6), 818.0 (ν_3), 800.3 (ν_5). (+)TOF *m/z* (amu): Calc. for (C₂₆H₂₀N₆O₈Gd)⁺: 702.0583. Found: 702.0579. Anal. Calc. for C₂₆H₂₈GdN₇O₁₅: C, 37.4; H,

3.4; N, 11.7. Found: C, 37.4; H, 3.6; N, 11.4.

2.2.3.6. [Tb(III)(Bzp1)₂(NO₃)₂]NO₃·3 H₂O (TbBzp1**).** The compound **TbBzp1** was synthesized following the procedure described in Section 2.2.3. from 107.73 mg of Tb(III)(NO₃)₃·6 H₂O (0.2378 mmol) and 100 mg of **Bzp1** (0.4757 mmol). A yellow product was obtained with a yield of 90.6% (0.1766 g, Mp 196 °C). FT-IR (ATR, ν cm⁻¹): 3065.8 (N–H), 3225.8 (O–H), 1625.0, 1610.0, 1561.4 (C=C)_{arom}, 1625.0 (C=N), 1289.9 (C–N), 1241.3 (C–O), 750.8 (C–H)_{arom}; NO₃ bands: 1459.0 (ν_1), 1390.1 (ν_0), 1289.9 (ν_4), 1022.0 (ν_2), 830.0 (ν_6), 814.3 (ν_3), 799.2 (ν_5). (+)TOF *m/z* (amu): Calc. for (C₂₆H₂₀N₆O₈Tb)⁺: 703.0596. Found: 703.0601. Anal. Calc. for C₂₆H₂₆TbN₇O₁₄: C, 38.1; H, 3.2; N, 12.0. Found: C, 37.8; H, 3.5; N, 11.8.

2.2.3.7. [Dy(III)(Bzp1)₂(NO₃)₂]NO₃·4 H₂O (DyBzp1**).** The compound **DyBzp1** was synthesized following the procedure described in Section 2.2.3. from 108.58 mg of Dy(III)(NO₃)₃·6 H₂O (0.2378 mmol) and 100 mg of **Bzp1** (0.4757 mmol). A yellow product was obtained with a yield of 86.8% (0.1737 g, Mp 247 °C). FT-IR (ATR, ν cm⁻¹): 3035.9 (N–H), 3250.0 (O–H), 1622.7, 1608.7, 1558.5, 1498.7 (C=C)_{arom}, 1622.7 (C=N), 1307.1 (C–N), 1242.1 (C–O), 751.7 (C–H)_{arom}; NO₃ bands: 1410.0 (ν_1), 1386.8 (ν_0), 1242.2 (ν_4), 1020.0 (ν_2), 840.0 (ν_6), 817.0 (ν_3), 798.0 (ν_5). (+)TOF *m/z* (amu): Calc. for (C₂₆H₂₀N₆O₈Dy)⁺: 708.0634. Found: 708.0628. Anal. Calc. for C₂₆H₂₈DyN₇O₁₅: C, 37.1; H, 3.4; N, 11.7. Found: C, 37.2; H, 3.8; N, 11.3.

2.2.3.8. [La(III)(Bzp2)₂(NO₃)₂]NO₃·4 H₂O (LaBzp2**).** The compound **LaBzp2** was synthesized following the procedure described in Section 2.2.3. from 96.56 mg of La(III)(NO₃)₃·6 H₂O (0.2230 mmol) and 100 mg of **Bzp2** (0.4460 mmol). A pink product was obtained with a yield of 87.8% (0.1655 g, Mp 246 °C). FT-IR (ATR, ν cm⁻¹): 3150.0 (N–H), 3200.0 (O–H), 1625.3, 1600.0, 1561.5, 1483.9 (C=C)_{arom}, 1625.3 (C=N), 1299.3 (C–N), 1242.8 (C–O), 743.8 (C–H)_{arom}; NO₃ bands: 1408.2 (ν_1), 1395.0 (ν_0), 1241.9 (ν_4), 1042.2 (ν_2), 849.7 (ν_6), 820.0 (ν_3), 805.8 (ν_5). (+)TOF *m/z* (amu): Calc. for (C₂₈H₂₄N₆O₈La)⁺: 711.0719. Found: 711.0723. Anal. Calc. for C₂₈H₃₂LaN₇O₁₅: C, 39.8; H, 3.8; N, 11.6. Found: C, 39.6; H, 4.2; N, 11.5.

2.2.3.9. [Nd(III)(Bzp2)₂(NO₃)₂]NO₃·4 H₂O (NdBzp2**).** The compound **NdBzp2** was synthesized following the procedure described in Section 2.2.3. from 97.75 mg of Nd(III)(NO₃)₃·6 H₂O (0.2230 mmol) and 100 mg of **Bzp2** (0.4460 mmol). A pink product was obtained with a yield of 86.9% (0.1649 g, Mp 189 °C). FT-IR (ATR, ν cm⁻¹): 3200.0 (N–H), 3300.0 (O–H), 1625.3, 1600.0, 1561.1, 1487.6 (C=C)_{arom}, 1625.3 (C=N), 1300.7 (C–N), 1242.9 (C–O), 743.8 (C–H)_{arom}; NO₃ bands: 1403.9 (ν_1), 1376.4 (ν_0), 1243.0 (ν_4), 1043.1 (ν_2), 850.0 (ν_6), 830.0 (ν_3), 804.6 (ν_5). (+)TOF *m/z* (amu): Calc. for (C₂₈H₂₄N₆O₈Nd)⁺: 714.0733. Found: 714.0737. Anal. Calc. for C₂₈H₃₂NdN₇O₁₅: C, 39.5; H, 3.8; N, 11.5. Found: C, 39.8; H, 4.0; N, 11.2.

2.2.3.10. [Sm(III)(Bzp2)₂(NO₃)₂]NO₃·2 H₂O (SmBzp2**).** The compound **SmBzp2** was synthesized following the procedure described in Section 2.2.3. from 99.12 mg of Sm(III)(NO₃)₃·6 H₂O (0.2230 mmol) and 100 mg of **Bzp2** (0.4460 mmol). A pink product was obtained with a yield of 93.7% (0.1715 g, Mp 141 °C). FT-IR (ATR, ν cm⁻¹): 3200.0 (N–H), 3300.0 (O–H), 1625.7, 1600.0, 1560.2, 1487.9 (C=C)_{arom}; 1625.7 (C=N), 1314.1 (C–N), 1243.4 (C–O), 743.7 (C–H)_{arom}; NO₃ bands: 1402.9 (ν_1), 1375.9 (ν_0), 1242.8 (ν_4), 1043.8 (ν_2), 848.8 (ν_6), 822.4 (ν_3), 804.3 (ν_5). (+)TOF *m/z* (amu): Calc. for (C₂₈H₂₄N₆O₈Sm)⁺: 716.0776. Found: 716.0779. Anal. Calc. for C₂₈H₂₈SmN₇O₁₃: C, 41.0; H, 3.4; N, 11.9. Found: C, 41.3; H, 3.2; N, 11.9.

2.2.3.11. [Eu(III)(Bzp2)₂(NO₃)₂]NO₃·5 H₂O (EuBzp2**).** The compound **EuBzp2** was synthesized following the procedure described in Section 2.2.3. from 95.46 mg of Eu(III)(NO₃)₃·5 H₂O (0.2230 mmol) and

100 mg of **Bzp2** (0.4460 mmol). A pink product was obtained with a yield of 85.2% (0.1666 g, Mp 247 °C). FT-IR (ATR, ν cm⁻¹): 3236.3 (N–H), 3410.2 (O–H), 1625.9, 1612.8, 1584.4, 1560.4 (C=C)_{arom}, 1625.9 (C=N), 1300.2 (C–N), 1243.0 (C–O), 744.8 (C–H)_{arom}; NO₃ bands: 1403.9 (ν_1), 1376.4 (ν_0), 1242.8 (ν_4), 1044.3 (ν_2), 849.2 (ν_6), 822.3 (ν_3), 803.1 (ν_5). (+)TOF *m/z* (amu): Calc. for (C₂₈H₂₄N₆O₈Eu)⁺: 725.0868. Found: 725.0873. Anal. Calc. for C₂₈H₃₄EuN₇O₁₆: C, 38.4; H, 3.9; N, 11.2. Found: C, 38.2; H, 3.7; N, 11.0.

2.2.3.12. [*Gd(III)(Bzp2)*]₂(NO₃)₂][NO₃]₃·3 H₂O (**GdBzp2**). The compound **GdBzp2** was synthesized following the procedure described in Section 2.2.3. from 100.65 mg of Gd(III)(NO₃)₃·6 H₂O (0.2230 mmol) and 100 mg of **Bzp2** (0.4460 mmol). A pink product was obtained with a yield of 90.8% (0.1712 g, Mp 194 °C). FT-IR (ATR, ν cm⁻¹): 3100.0 (N–H), 3355.1 (O–H), 1624.4, 1609.8, 1561.2, 1485.3 (C=C)_{arom}, 1624.4 (C=N), 1296.3 (C–N), 1242.8 (C–O), 743.8 (C–H)_{arom}; NO₃ bands: 1402.8 (ν_1), 1375.4 (ν_0), 1242.6 (ν_4), 1041.9 (ν_2), 848.8 (ν_6), 822.4 (ν_3), 807.0 (ν_5). (+)TOF *m/z* (amu): Calc. for (C₂₈H₂₄N₆O₈Gd)⁺: 730.0896. Found: 730.0901. Anal. Calc. for C₂₈H₃₀GdN₇O₁₄: C, 39.8; H, 3.6; N, 11.6. Found: C, 39.7; H, 3.8; N, 11.7.

2.2.3.13. [*Tb(III)(Bzp2)*]₂(NO₃)₂][NO₃]₃·3 H₂O (**TbBzp2**). The compound **TbBzp2** was synthesized following the procedure described in Section 2.2.3. from 101.02 mg of Tb(III)(NO₃)₃·6 H₂O (0.2230 mmol) and 100 mg of **Bzp2** (0.4460 mmol). A pink product was obtained with a yield of 90.8% (0.1716 g, Mp 249 °C). FT-IR (ATR, ν cm⁻¹): 3233.3 (N–H), 3355.1 (O–H), 1625.2, 1612.1, 1561.3, 1487.7 (C=C)_{arom}, 1625.2 (C=N), 1314.1 (C–N), 1242.9 (C–O), 743.8 (C–H)_{arom}; NO₃ bands: 1403.5 (ν_1), 1375.9 (ν_0), 1242.8 (ν_4), 1043.2 (ν_2), 849.7 (ν_6), 822.9 (ν_3), 804.2 (ν_5). (+)TOF *m/z* (amu): Calc. for (C₂₈H₂₄N₆O₈Tb)⁺: 731.0909. Found: 731.0913. Anal. Calc. for C₂₈H₃₀TbN₇O₁₄: C, 39.7; H, 3.6; N, 11.6. Found: C, 39.5; H, 3.5; N, 11.9.

2.2.3.14. [*Dy(III)(Bzp2)*]₂(NO₃)₂][NO₃]₃·4 H₂O (**DyBzp2**). The compound **DyBzp2** was synthesized following the procedure described in Section 2.2.3. from 101.82 mg of Dy(III)(NO₃)₃·6 H₂O (0.2230 mmol) and 100 mg of **Bzp2** (0.4460 mmol). A pink product was obtained with a yield of 88.0% (0.1706 g, Mp 192 °C). FT-IR (ATR, ν cm⁻¹): 3200.0 (N–H), 3413.0 (O–H), 1625.2, 1561.3, 1487.5 (C=C)_{arom}, 1625.2 (C=N), 1303.6 (C–N), 1243.4 (C–O), 745.1 (C–H)_{arom}; NO₃ bands: 1403.4 (ν_1), 1376.0 (ν_0), 1242.9 (ν_4), 1042.6 (ν_2), 849.7 (ν_6), 822.4 (ν_3), 806.2 (ν_5). (+)TOF *m/z* (amu): Calc. for (C₂₈H₂₄N₆O₈Dy)⁺: 736.0947. Found: 736.0954. Anal. Calc. for C₂₈H₃₂DyN₇O₁₅: C, 38.7; H, 3.7; N, 11.3. Found: C, 38.7; H, 3.3; N, 11.1.

2.3. Cytotoxicity assays

2.3.1. Cell lines

Cytotoxic studies were executed in three cell lines: HeLa (ATCC CLL-2) cervical adenocarcinoma epithelial, NIH-3T3 (ATCC CRL-1658) embryonic fibroblast and J774A.1 (ATCC TIB-67) monocyte macrophages. Cells were placed in DMEM (Dulbecco's modified Eagle's medium). The medium was supplemented with L-glutamine (2 mM) and 10% fetal bovine serum. The cells were incubated at 37 °C for six days, in 5% CO₂ and 95% relative humidity.

2.3.2. Sulphorhodamine (SRB) assay

Biological studies were performed on a NuAire IR autoflow 5500 water-jacketed automatic CO₂ incubator. The photometric microplates were read in a photometer for Thermo Scientific Multiskan EX microplates.

96-well microtiter plates were used, where the cells were seeded (5 × 10⁶ cells per well) and allowed to proliferate for 48 h in dulbecco's modified eagle medium (DMEM) containing 10% fetal bovine serum. The two ligands and their fourteen Ln(III) complexes were studied using different concentrations (1, 10, 25, 50, 100 μM) in 1% dimethyl

sulphoxide (DMSO) and were applied to the cell monolayer by duplicate. The complexes that showed moderate selectivity were also studied at higher concentrations (150, 200, 250, μM). 1% Sodium dodecyl sulfate (SDS) was employed as positive control of cell death (0% of cell viability) and 1% DMSO was used as the negative control (100% of cell viability). The incubation was carried out at 37 °C with 5% CO₂ for 72 h, and subsequently the cell growth was evaluated by the sulphorhodamine B assay (SRB).

The SRB assay was carried out as previously described by Papazisis et al. [82]. Briefly, the culture medium was suctioned prior to fixation and 50 μL of 10% cold trichloroacetic acid (4 °C) was gently added to the wells. Microplates were left for 30 min at 4 °C, washed five times with deionized water and left to dry at room temperature for at least 24 h. Subsequently, 50 μL 0.4% (w/v) SRB (Sigma) in 1% acetic acid solution was added to each well and left at room temperature for 20 min. The SRB was removed and the plates were washed five times with 1% acetic acid before air-drying. The bound SRB was dissolved with 50 μL of 10 mM non-buffered Tris-base solution, and microplates were placed on microplate shaker for at least 10 min. Absorbance was read at 530 nm by subtracting the 620 nm background measurement. The results obtained define the viability percentage. The half maximal inhibitory concentration (IC₅₀) was expressed as the concentration that reduces the optical density (OD₅₃₀) of treated cells to 50% with respect of the untreated cells. The IC₅₀ value was established as the concentration of the Ln(III) complex where percent inhibition was equal to 50% and was the mean of at least two independent experiments.

2.3.3. Erythrocytes lysis assay

The procedure reported by Ramos-Ligonio et al., in 2012 was utilized with some modifications that are mentioned below. Human blood was extracted from a healthy patient by peripheral venous puncture. Subsequently, each of the samples was centrifuged, separating the plasma and blood cells. The red blood cells were rinsed twice with PBS (phosphate buffer solution, pH 7.4). A 2% suspension of human red blood cells was prepared and 200 μL were incubated at 37 °C for 6 h with the tested compounds: **NdBzp2**, **GdBzp2**, **TbBzp2** and **DyBzp2**, at different concentrations (1, 10, 25, 50, 100 μM). All samples were centrifuged at 1000 ×g for 10 min. The absorbance of the supernatant was estimated at 540 nm. Haemolysis inhibition was calculated according to the equation described below [83].

$$\text{Haemolysis inhibition (\%)} = \frac{A_p - A_s}{A_p - A_n} \times 100$$

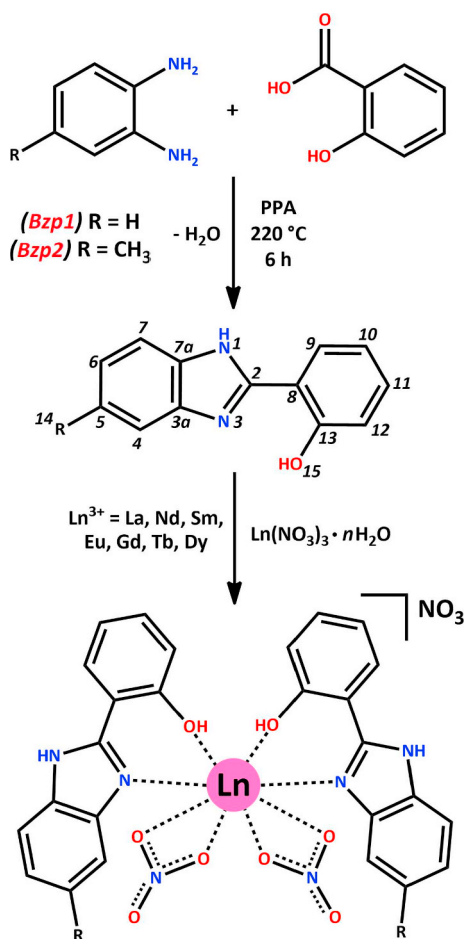
where *A_s*, *A_p* and *A_n* were the absorbance of the test sample, the positive control (1% Triton X-100), and the negative control (1% DMSO) respectively. These results were the mean of at least two independent experiments.

2.3.4. Statistical analysis

Two replicates were performed for each experiment in each of the conditions tested, and to ensure reproducibility the experiments were made twice. In the statistical analysis, the Dunnett tests and the one-way analysis of variance (ANOVA) were employed and the statistical significance was defined as *p* < 0.05. Statistical analysis for the calculation of the IC₅₀, as well as the comparison of cell growth inhibition curves, were performed with the GraphPad Prism version 5.04 program applying a non-linear regression analysis [84].

2.4. Computational details

The optimized geometries and vibrational modes of the La(III) complexes were obtained using the hybrid method B3LYP with the pseudopotential LANL2DZ [85–87] employing Gaussian 03 software package [88]. All the frequencies presented positive values, so we obtained equilibrium conformers for the considered complexes. The analysis of the IR vibration frequencies for the La(III) complexes was



Scheme 1. Reaction of the benzimidazolyl-phenol ligands with Ln(III)(NO₃)₃·nH₂O.

performed using the same level of theory (B3LYP/LANL2DZ), comparing theoretical *versus* experimental frequencies using vibrational scale factors [89,90]. The graphical results were obtained with the programs: Chemcraft version 1.8 (compilation 536b) [91] and Diamond version 4.5.1 [92].

3. Results and discussion

3.1. Synthesis of the compounds

Fourteen novel complexes of formula [Ln(III)(L)₂(NO₃)₂]NO₃·nH₂O (L = **Bzp1** or **Bzp2**; Ln(III) = La, Nd, Sm, Eu, Gd, Tb, Dy) were synthesized in high yields from the reaction between the chromophores (**Bzp1** or **Bzp2**) and seven Ln(III)(NO₃)₃·nH₂O in a [2:1] stoichiometry, **Scheme 1**. The Ln(III) complexes are reported for the first time in this article; however, the synthesis of the ligands (**Bzp1** and **Bzp2**) had already been previously reported in the literature in different reaction conditions by different authors [10–50]. A proposed reaction mechanism for the synthesis of the chromophores is included in the supplementary information, **Scheme S1**. All Ln(III) complexes are completely soluble in solvents such as dimethyl sulfoxide, ethanol and methanol. In addition, they are partially soluble in solvents such as acetone, acetonitrile, chloroform, dichloromethane and water.

3.2. Spectroscopic studies of the compounds

The chemical structure of the chromophores (**Bzp1** and **Bzp2**) were confirmed by NMR at room temperature with DMSO-*d*₆, ¹H and ¹³C chemical shifts were unmistakably labelled by specific experiments,

such as: HETCOR, COSY and APT. Chemical shift, integration and constant couplings were not discussed here, since other authors had previously reported them [10–50].

The IR absorptions of the coordination complexes showed slight changes with respect to those of the ligands, indicating that they are coordinated to the lanthanides through iminic nitrogen and phenolic oxygen. The most representative stretching bands are: ν (C=N) ~ 1624 cm⁻¹, ν (C–N) ~ 1281 cm⁻¹ and ν (C–O) ~ 1241 cm⁻¹ for the complexes containing **Bzp1**; ν (C=N) ~ 1625 cm⁻¹, ν (C–N) ~ 1300 cm⁻¹ and ν (C–O) ~ 1242 cm⁻¹ for the complexes containing **Bzp2**. The strong vibration due to ν (O–H) bond was observed between 3200 and 3400 cm⁻¹, confirming that the hydroxyl groups do not deprotonate. The spectra of the compounds displayed the characteristic absorptions of the bidentate NO₃ groups (C_{2v}): ~ 1458 cm⁻¹ (ν_1), ~ 1289 cm⁻¹ (ν_4), ~ 1022 cm⁻¹ (ν_2) and ~ 815 cm⁻¹ (ν_3) for the complexes containing **Bzp1**; ~ 1408 cm⁻¹ (ν_1), ~ 1242 cm⁻¹ (ν_4), ~ 1043 cm⁻¹ (ν_2) and ~ 822 cm⁻¹ (ν_3) for the complexes containing **Bzp2**. The difference in wave number between the two most intense absorptions of the bidentate NO₃ group (ν_1 and ν_4) provided values between 160 and 170 cm⁻¹, confirming that two NO₃ groups (C_{2v}) are coordinated to the Ln(III) ions in a bidentate mode [51–53,93]. The intense stretching band due to ν_4 (NO₃ group) overlaps the less intense stretching bands of ν (C–N) and ν (C–O). In comparison to an unbound NO₃ group (D_{3h}), the characteristic absorptions can be seen in the spectra of the complexes: ~ 1393 cm⁻¹ (ν_0), ~ 840 cm⁻¹ (ν_6) and ~ 798 cm⁻¹ (ν_5) for the complexes containing **Bzp1**; ~ 1376 cm⁻¹ (ν_0), ~ 849 cm⁻¹ (ν_6) and ~ 804 cm⁻¹ (ν_5) for the complexes containing **Bzp2**, **Table 1**. These three less intense bands denote that one NO₃ group (D_{3h}) is counterion in the Ln(III) complexes. Therefore, the results obtained by FT-IR agree with the experimental evidence obtained by molar conductivity measured in methyl alcohol, characteristic for 1:1 electrolytes, **Table 2**.

The solid-state emission, excitation and absorption spectra at room temperature of the chromophores (**Bzp1** and **Bzp2**) were recorded and the latter two are shown in **Fig. 1**. The excitation spectra showed two bands at 348 nm (28,735 cm⁻¹) and 397 nm (25,189 cm⁻¹) for **Bzp1**, 347 nm (28,818 cm⁻¹) and 396 nm (25,252 cm⁻¹) for **Bzp2**. The absorption spectra of the Ln(III) complexes presented a broad band in the UV-region similar to the absorption maxima of the ligands. The Nd(III), Sm(III) and Dy(III) intraconfigurational 4*f*–4*f* transitions were observed in the diffuse reflectance for the complexes with **Bzp1** and **Bzp2**, the assignments are displayed in **Table 3** and **Fig. 2**. The emission spectra of the ligands showed the band assigned to the ¹S₁ → ¹S₀ transition: 455 nm (21,978 cm⁻¹) for **Bzp1**, and 440 nm (22,727 cm⁻¹) for **Bzp2**. The maximum emission does not change for each ligand, whether the sample is excited at 348 or 397 nm for **Bzp1**, or either at 347 or 396 nm for **Bzp2**; however, the intensity of the luminescence varies upon the

Table 1
NO₃ stretching bands (cm⁻¹) for all Ln(III) complexes.

Compound	NO ₃ ⁻ , C _{2v} (cm ⁻¹)				NO ₃ ⁻ , D _{3h} (cm ⁻¹)			
	ν_1	ν_4	ν_2	ν_3	$\nu_1-\nu_4$	ν_0	ν_6	ν_5
LaBzp1	1458.4	1289.5	1022.5	815.3	169	1393.4	840.0	798.7
NdBzp1	1457.1	1289.3	1022.3	815.2	168	1393.8	839.7	799.1
SmBzp1	1459.8	1290.1	1022.3	818.9	170	1392.6	839.2	798.6
EuBzp1	1458.7	1289.7	1022.2	817.6	169	1392.8	835.0	798.2
GdBzp1	1462.5	1304.9	1022.0	818.0	158	1401.3	839.9	800.3
TbBzp1	1459.0	1289.9	1022.0	814.3	169	1390.1	830.0	799.2
DyBzp1	1410.0	1242.2	1020.0	817.0	168	1386.8	840.0	798.0
LaBzp2	1408.2	1241.9	1042.2	820.0	166	1395.0	849.7	805.8
NdBzp2	1403.9	1243.0	1043.1	830.0	161	1376.4	850.0	804.6
SmBzp2	1402.9	1242.8	1043.8	822.4	160	1375.9	848.8	804.3
EuBzp2	1403.9	1242.8	1044.3	822.3	161	1376.4	849.2	803.1
GdBzp2	1402.8	1242.6	1041.9	822.4	160	1375.4	848.8	807.0
TbBzp2	1403.5	1242.8	1043.2	822.9	161	1375.9	849.7	804.2
DyBzp2	1403.4	1242.9	1042.6	822.4	161	1376.0	849.7	806.2

Table 2
Effective magnetic moment and electrical conductivity in solution for all Ln(III) complexes.

Compound	μ_{eff} (B.M.)	$\mu\text{S/cm}$ (10^{-3} M)
<i>LaBzp1</i>	0	87.42
<i>NdBzp1</i>	3.55	82.73
<i>SmBzp1</i>	1.58	95.08
<i>EuBzp1</i>	3.42	91.13
<i>GdBzp1</i>	7.93	96.36
<i>TbBzp1</i>	9.66	95.07
<i>DyBzp1</i>	10.42	97.45
<i>LaBzp2</i>	0	89.77
<i>NdBzp2</i>	3.60	85.48
<i>SmBzp2</i>	1.42	93.34
<i>EuBzp2</i>	3.31	90.55
<i>GdBzp2</i>	7.97	95.33
<i>TbBzp2</i>	9.73	94.91
<i>DyBzp2</i>	10.54	96.25

excitation wavelength, as shown in Fig. 1. The spectra of most Ln(III) complexes obtained herein only show broad emission bands similar to those of the ligands, see Table 3. This result indicates that there is no energy transfer from either of the ligands to the metal ions.

3.3. Thermogravimetric analysis and magnetic susceptibility

The thermal stability of the compounds was determined by choosing a representative compound of each series of isostructural complexes derived from *Bzp1* and *Bzp2*. The selected compounds were the Nd(III) and Gd(III) derivatives respectively (*NdBzp1* and *GdBzp2*), the thermogravimetric analysis (TGA) data were obtained by gradually increasing the temperature 10 °C per minute. The thermograms of the Ln(III) complexes are listed in Table 4.

The complexes *NdBzp1* and *GdBzp2* undergo a similar disintegration, which is carried out in three steps. The first step occurs in the range of 70–105 °C and corresponds to the loss of three water molecules of the crystal lattice. The second and the third step of the decomposition correspond to the loss of two NO₃ coordinated to the Ln(III) ion and one NO₃ of the crystal lattice in the temperature ranges of 175–230 °C and 230–275 °C respectively. Finally, the Ln(III) complexes decompose completely losing the benzimidazolyl-phenol ligands in the temperature range of 300–500 °C and the residues are rare earth oxides. The results showed a thermal stability similar to other compounds reported in the literature, and this discard the presence of water molecules coordinated to the Ln(III) ion [55–57,72–74].

The effective magnetic moments of the Ln(III) complexes were determined by the Gouy's method and correspond to the anticipated values for the Ln(III) ions [51–54], see Table 2. The values of the experimental magnetic moment indicate that the complexes of La(III) are

diamagnetic, due to the absence of electrons in the 4*f* orbitals, while the other coordination complexes are paramagnetic, as expected. The magnetic moment values obtained agree with those described for analogous complexes previously reported, confirming the non-participation of the 4*f* electrons in the coordination bonds, due to the shielding facilitated by the 5*s*²5*p*⁶ electrons [55,72].

3.4. Cytotoxic activity of the compounds

The ability of the fourteen complexes and the two ligands to inhibit cell growth was evaluated by *in vitro* assay performed on HeLa (cervical adenocarcinoma epithelial) cells. These cells are currently studied as potential target of several cytotoxic metal complexes different from platinum, for example transition metals and rare earths. The cytotoxic effect on HeLa was evaluated using the SRB assay for all the compounds, comparing the results with those of two other cell lines: fibroblasts (NIH-3T3) and macrophages (J774A.1). The two ligands (*Bzp1* and *Bzp2*), all the Ln(III) complexes derived from *Bzp1* (with La, Nd, Sm, Eu, Gd, Tb and Dy), as well as three of the complexes derived from *Bzp2* (with La, Sm and Eu), showed cell viability lower than 50% for HeLa and NIH-3T3 mainly, indicating that these compounds are highly cytotoxic. Figs. S1–S4.

Four compounds derived from *Bzp2* (*NdBzp2*, *GdBzp2*, *TbBzp2* and *DyBzp2*) showed interesting cytotoxic behavior. Three of them (*GdBzp2*, *TbBzp2* and *DyBzp2*) were moderately selective against HeLa cells and did not cause death of NIH-3T3 and J774A.1 cells. The above is an important advantage, since these compounds could be employed as adjuvants in chemotherapy treatments, as long as their activity was maintained *in vivo*. They would not induce tissue damage and would keep the macrophage population intact, decreasing the side effects shown by the treatments currently employed. It was observed that the cytotoxic effect of these three complexes in the HeLa cell line does not show a dose-dependent behavior. In addition, *NdBzp2* was not selective and lysed HeLa and J774A.1 cells indistinctly, which is not convenient, since it destroys both adenocarcinoma cells and defense cells, Fig. 3. The stability in solution of these four complexes (*NdBzp2*, *GdBzp2*, *TbBzp2* and *DyBzp2*) was evaluated in order to support the results of cytotoxicity. The details are shown in the supplementary information. Tables S1–S4.

According to the selectivity shown, an effective response was observed for *NdBzp2*, *GdBzp2*, *TbBzp2* and *DyBzp2* in HeLa cells, while the effect was smaller in the NIH-3T3 and J774A.1 cell lines. It is important to note that the four compounds that displayed cytotoxic activity in the SRB assay are functionalized in the C5 position, as in several commercial benzimidazole-derived drugs. The selectivity allows us to suppose that the activity shown would favor the activation of the immune system, capable of attacking only damaged tumor cells in the same way that occurs *in vivo*; however, this could only be confirmed by evaluating the effects of the Ln(III) complexes in the cell cycle and their

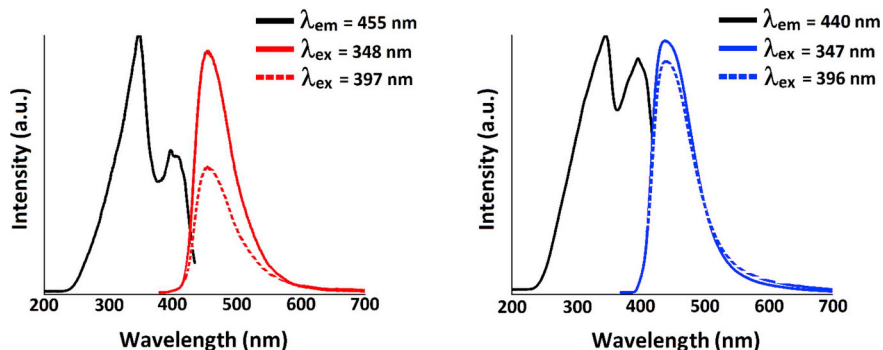


Fig. 1. Solid-state excitation and emission spectra of the chromophores *Bzp1* (left) and *Bzp2* (right).

Table 3
Absorption and emission data for all Ln(III) complexes.

Compound	Absorption λ (nm)	Emission λ (nm)	Compound	Absorption λ (nm)	Emission λ (nm)
L1	362, $^1S_1 \leftarrow ^1S_0$	455, $^1S_1 \rightarrow ^1S_0$	L2	368, $^1S_1 \leftarrow ^1S_0$	440, $^1S_1 \rightarrow ^1S_0$
LaBzp1	364, $^1S_1 \leftarrow ^1S_0$	393, $^1S_1 \rightarrow ^1S_0$	LaBzp2	371, $^1S_1 \leftarrow ^1S_0$	420, $^1S_1 \rightarrow ^1S_0$
NdBzp1	361, $^1S_1 \leftarrow ^1S_0$	395, $^1S_1 \rightarrow ^1S_0$	NdBzp2	367, $^1S_1 \leftarrow ^1S_0$	431, $^1S_1 \rightarrow ^1S_0$
	742, $^4F_{7/2}, ^4S_{3/2} \leftarrow ^4I_{9/2}$			741, $^4F_{7/2}, ^4S_{3/2} \leftarrow ^4I_{9/2}$	
	797, $^4F_{5/2}, ^2H_{9/2} \leftarrow ^4I_{9/2}$			797, $^4F_{5/2}, ^2H_{9/2} \leftarrow ^4I_{9/2}$	
	865, $^4F_{3/2} \leftarrow ^4I_{9/2}$			863, $^4F_{3/2} \leftarrow ^4I_{9/2}$	
SmBzp1	364, $^1S_1 \leftarrow ^1S_0$	438, $^1S_1 \rightarrow ^1S_0$	SmBzp2	371, $^1S_1 \leftarrow ^1S_0$	441, $^1S_1 \rightarrow ^1S_0$
	941, $^6F_{11/2} \leftarrow ^6H_{5/2}$			938, $^6F_{11/2} \leftarrow ^6H_{5/2}$	
	1086, $^6F_{9/2} \leftarrow ^6H_{5/2}$			1079, $^6F_{9/2} \leftarrow ^6H_{5/2}$	
EuBzp1	367, $^1S_1 \leftarrow ^1S_0$	437, $^1S_1 \rightarrow ^1S_0$	EuBzp2	378, $^1S_1 \leftarrow ^1S_0$	438, $^1S_1 \rightarrow ^1S_0$
GdBzp1	383, $^1S_1 \leftarrow ^1S_0$	446, $^1S_1 \rightarrow ^1S_0$	GdBzp2	367, $^1S_1 \leftarrow ^1S_0$	401, $^1S_1 \rightarrow ^1S_0$
TbBzp1	385, $^1S_1 \leftarrow ^1S_0$	445, $^1S_1 \rightarrow ^1S_0$	TbBzp2	378, $^1S_1 \leftarrow ^1S_0$	422, $^1S_1 \rightarrow ^1S_0$
DyBzp1	362, $^1S_1 \leftarrow ^1S_0$	447, $^1S_1 \rightarrow ^1S_0$	DyBzp2	376, $^1S_1 \leftarrow ^1S_0$	426, $^1S_1 \rightarrow ^1S_0$
	798, $^6F_{5/2} \leftarrow ^6H_{15/2}$			797, $^6F_{5/2} \leftarrow ^6H_{15/2}$	
	903, $^6F_{7/2} \leftarrow ^6H_{15/2}$			900, $^6F_{7/2} \leftarrow ^6H_{15/2}$	
	1098, $^6F_{9/2}, ^6H_{7/2} \leftarrow ^6H_{15/2}$			1095, $^6F_{9/2}, ^6H_{7/2} \leftarrow ^6H_{15/2}$	

possible immunomodulatory activity.

In order to evaluate the cytotoxicity of the four complexes in detail, their IC₅₀ values were determined. The IC₅₀ value (half maximal inhibitory concentration), expressed in μ M, is the concentration of the Ln(III) complex that affords a 50% reduction in cell growth and the results were displayed in Table 5. The IC₅₀ value of the new complexes in HeLa cells is higher compared to the IC₅₀ of some commercial anticancer agents, such as noscapine (22 μ M), estramustine (1.5–3.0 μ M) and cisplatin (8 μ M) [55–57]. However, their cytotoxic effect is equal or better than some shown by other previously reported Ln(III) complexes [60–62,67–74]. This improvement can be attributed to the presence of the benzimidazolic group in the compounds synthesized herein. In addition, with the exception of cisplatin, there is little information on how metal drugs work against cancer, but it is clear that the presence of different metal ions favors the cellular response [68]. Ln(III) ions can suppress the absorption of Ca(II), Mg(II), Fe(II) or Mn(II), thus inhibiting Ca(II)-dependent enzymes, or else inhibiting the formation of free radicals or ROS, as previously mentioned [69–75,94]. However, additional experiments would be necessary to support this assumption.

3.5. Percentage of haemolysis inhibition of the compounds

It is important to note that when looking for new compounds that have a potential anticancer effect, these must have high cytotoxic selectivity and should not cause damage to mammalian host cells. In order to validate the selectivity in the cytotoxic assay, a cytotoxicity test was implemented in human red blood cells. The results show that the Ln(III) complexes used (**NdBzp2**, **GdBzp2**, **TbBzp2** and **DyBzp2**) do not affect the red blood cells in the concentrations in which they cause cytotoxicity in the HeLa cell line. These four compounds did not show cytotoxic effect against human erythrocytes. In addition, the solution of

Table 4
Thermogravimetric data for **NdBzp1** and **GdBzp2**.

Compound	Temperature range (°C)	% Weight loss obs. (calcd)	Process
NdBzp1	70–105	6.95 (6.71)	Loss of three lattice H ₂ O
	175–230	7.85 (7.70)	Loss of one lattice NO ₃
	230–300	14.88 (15.40)	Loss of two coord. NO ₃
	> 300	51.93 (52.24)	Loss of organic moiety
GdBzp2	70–105	6.50 (6.37)	Loss of three lattice H ₂ O
	175–230	6.82(7.31)	Loss of one lattice NO ₃
	230–300	14.90 (14.62)	Loss of two coord. NO ₃
	> 300	52.55 (52.90)	Loss of organic moiety

1% Triton X-100 exhibited 100% haemolysis, whereas 1% DMSO did not cause haemolysis. Fig. 4.

3.6. Optimized structures and vibrational frequencies calculated by density functional theory (DFT)

The structural arrangement and geometry were determined for a representative compound of each series of the isostructural complexes derived from **Bzp1** and **Bzp2**. The compounds selected were **LaBzp1** and **LaBzp2**. DFT calculations indicate that coordination complexes contain an octacoordinated La(III) ion bonded to two bidentate ligands (**Bzp1** and **Bzp2**) and two bidentate nitrate ions, with a distorted dodecahedral geometry (snub disphenoid) commonly observed for La(III) ions. The local coordination environment around the La(III) ion is depicted in Fig. 5, where five of the six oxygen atoms are placed in the same plane, while the two nitrogen atoms are placed in the apical positions of the dodecahedron. The data obtained by DFT calculations allow proposing a structure for the Ln(III) complexes, supported by

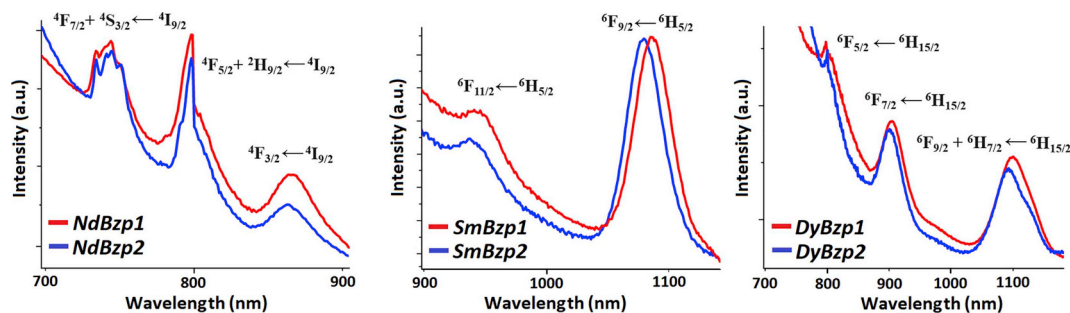


Fig. 2. Diffuse reflectance spectra of the complexes with Nd(III), Sm(III) and Dy(III). See Table 3 for the assignment of the 4f–4f transitions.

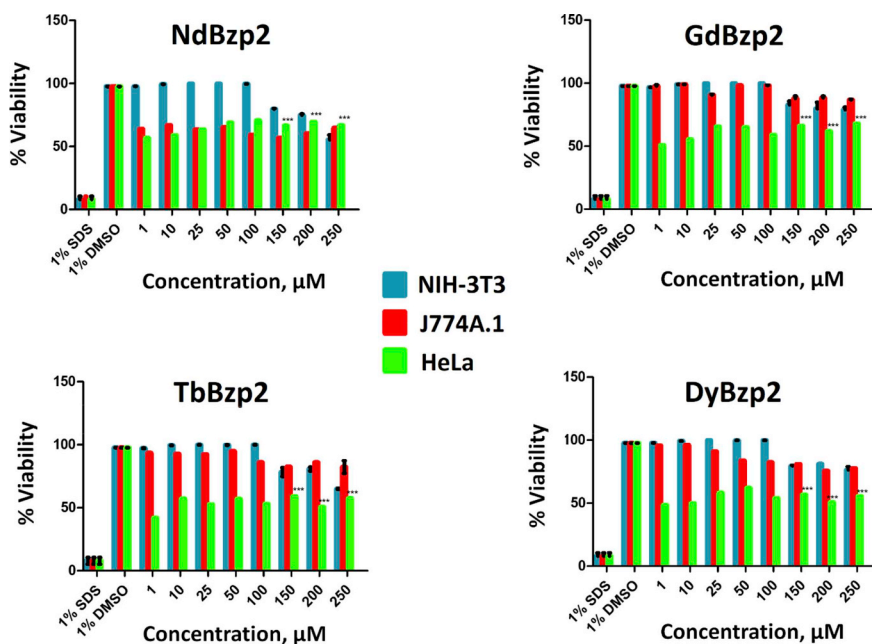


Fig. 3. Effect of Ln(III) complexes on cell viability. The NIH-3T3, J774A.1 and HeLa cell lines were cultured with different concentrations of *NdBzp2*, *GdBzp2*, *TbBzp2* and *DyBzp2*. 1% SDS corresponds to 0% viability, while 1% DMSO corresponds to 100% viability. Values shown are the mean SD of duplicate cultures. The data are representative of the results of two independent experiments. *Displays statistically significant differences (Dunnet, $p < 0.001$).

Table 5
Half-maximal inhibitory concentration (IC_{50}) for *NdBzp2*, *GdBzp2*, *TbBzp2* and *DyBzp2*.

Compound	Cell lines, IC_{50} (μM) ^a		
	NIH-3T3	J774A.1	HeLa
<i>NdBzp2</i>	16.01 \pm 2.79	57.16 \pm 6.59	30.90 \pm 4.01
<i>GdBzp2</i>	85.30 \pm 3.35	24.92 \pm 4.47	13.54 \pm 1.96
<i>TbBzp2</i>	72.85 \pm 3.64	84.13 \pm 3.74	7.90 \pm 1.21
<i>DyBzp2</i>	59.26 \pm 5.43	67.99 \pm 5.36	13.00 \pm 4.01

^a IC_{50} values are presented as the mean \pm standard deviation of the mean from two separate experiments.

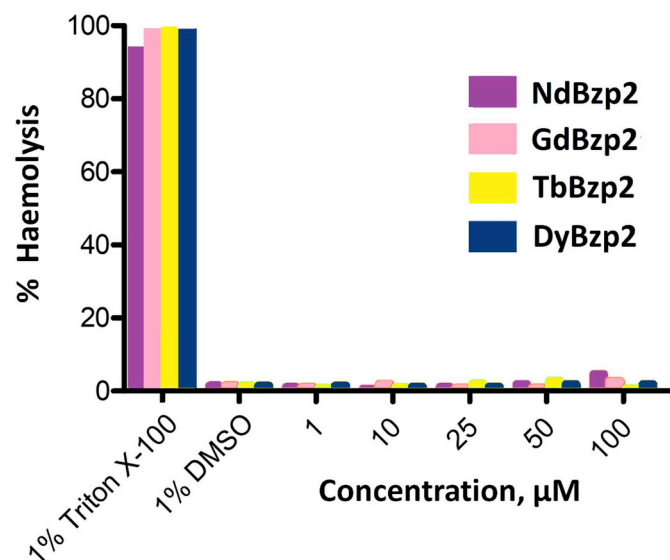


Fig. 4. Percentage of haemolysis inhibition in the interaction of the *NdBzp2*, *GdBzp2*, *TbBzp2* and *DyBzp2* complexes in different concentrations with human erythrocytes. 1% DMSO corresponds to 0% haemolysis, while 1% Triton X-100 corresponds to 100% haemolysis. The data are representative of the results of two independent experiments.

analytical and spectroscopic evidence.

The calculated IR spectra of the complexes displayed the vibration frequencies of the bidentate NO_3 groups: 1489 cm^{-1} (ν_1), 1267 cm^{-1} (ν_4), 1098 cm^{-1} (ν_2) and 809 cm^{-1} (ν_3) for *LaBzp1*; 1488 cm^{-1} (ν_1), 1267 cm^{-1} (ν_4), 1097 cm^{-1} (ν_2) and 808 cm^{-1} (ν_3) for *LaBzp2*. In addition, the vibration frequencies of the anionic NO_3 groups were showed in: 1403 cm^{-1} (ν_0), 841 cm^{-1} (ν_6) and 798 cm^{-1} (ν_5) for *LaBzp1*; 1398 cm^{-1} (ν_0), 850 cm^{-1} (ν_6) and 799 cm^{-1} (ν_5) for *LaBzp2*.

4. Conclusions

An efficient and simple method for the synthesis of [Ln(III)(L)₂(NO₃)₂]NO₃ \cdot *n*-H₂O complexes with benzimidazolyl-phenol ligands is discussed herein. The *Bzp1* and *Bzp2* chromophores and the Ln(III) complexes were identified by several analytical and spectroscopic methods. The comparative analysis of the FT-IR spectra of the chromophores and their Ln(III) complexes shows that the stretching bands assigned to the organic fragment move when they coordinate with the Ln(III) ions, confirming the bidentate nature of the ligands. All compounds are ionic. The TGA data showed that two NO_3 groups are coordinated of bidentate manner to the Ln(III) ion and are part of the coordination sphere, while one NO_3 group is outside the coordination sphere and compensates the charge of the complex. In addition, a decomposition process of the Ln(III) complexes was observed in three stages.

The cytotoxic activity of the Ln(III) complexes and their benzimidazolyl-phenol ligands was tested by the SRB assay in order to have new drugs candidates against cancer. Cell cytotoxicity studies of these complexes on HeLa, NIH-3T3 and J774A.1 cells indicate that they have the potential to act as effective anticancer drugs. The results indicate that only four (*NdBzp2*, *GdBzp2*, *TbBzp2* and *DyBzp2*) of the fourteen rare earth complexes possess different degrees of inhibition in HeLa cells. The Ln(III) complexes (*GdBzp2*, *TbBzp2* and *DyBzp2*) exhibited cytotoxic activity towards cervical adenocarcinoma epithelial cells (HeLa), and showed a minor cytotoxic effect in structure/support cells (NIH-3T3) and defense cells (J774A.1), but only *TbBzp2* had lower IC_{50} values than cisplatin. The results obtained in this study provide an experimental basis for the development of new anticancer drugs based on rare earths with low cytotoxicity.

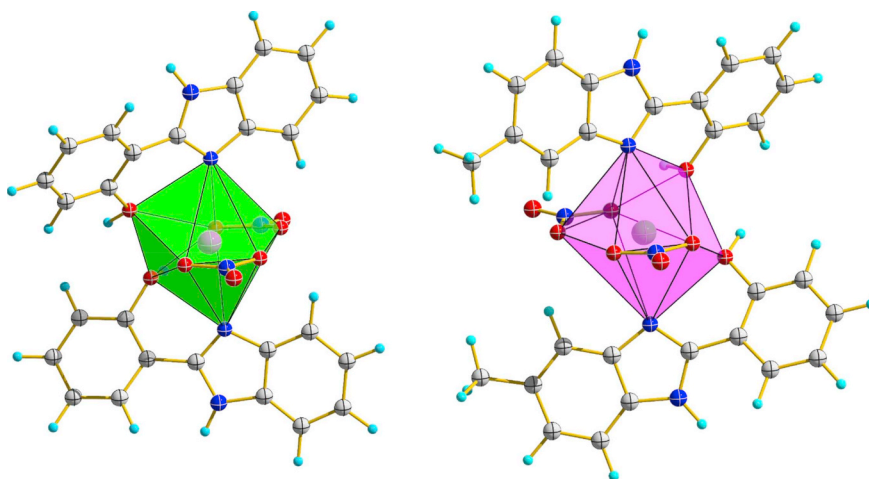


Fig. 5. Lowest energy optimized structures with symmetry C_2 of **LaBzp1** and **LaBzp2** by B3LYP/LANL2DZ.

Acknowledgements

We greatly appreciate the academic support of our institutions: UV, UNAM, and CINVESTAV-IPN, as well as the financial support of our projects: PRODEP/103.5/10595, CONACyT/CB/178851 and UNAM/DGAPA/PAPIIT/IN218917. We also appreciate the technical support: Maribel Rangel Rivera, Cristina Zúñiga Palacios and Sonia Araceli Sánchez Ruiz.

Appendix A. Supplementary data

Supplementary data to this article can be found online at <https://doi.org/10.1016/j.jinorgbio.2019.110842>.

References

- A. Tavman, N.M. Agh-Atabay, S. Guner, F. Gucin, B. Dulger, Investigation of Raman, FT-IR, EPR spectra and antimicrobial activity of 2-(5-H/Me/Cl-1H-benzimidazol-2-yl)phenol ligands and their $\text{Fe}(\text{NO}_3)_3$ complexes, *Transit Metal Chem* 32 (2) (2007) 172–179.
- A. Tavman, N.M. Agh-Atabay, A. Neshat, F. Gucin, B. Dulger, D. Hacıu, Structural characterization and antimicrobial activity of 2-(5-H/methyl-1H-benzimidazol-2-yl)-4-bromo/nitrophenol ligands and their $\text{Fe}(\text{NO}_3)_3$ complexes, *Transit Metal Chem* 31 (2) (2006) 194–200.
- A. Tavman, Synthesis, spectral characterization of 2-(5-methyl-1H-benzimidazol-2-yl)-4-bromo/nitro-phenols and their complexes with zinc(II) ion, and solvent effect on complexation, *Spectrochim. Acta A* 63A (2) (2006) 343–348.
- A. Tavman, B. Ulkuseven, Zinc(II) complexes of 2-(2-hydroxy-5-bromo/nitrophenyl)-5-methyl/chloro/nitro-1H-benzimidazoles, *Main Group Met Chem* 24 (4) (2001) 205–210.
- S.B. Garud, L.P. Shinde, Synthesis, characterization antimicrobial investigations of copper(II) complexes with some benzylbenzimidazole derivatives, *Res J Pharm Biol Chem Sci* 4 (4) (2013) 1285–1290.
- Y.-P. Tong, Y.-W. Lin, Synthesis, X-ray crystal structure, DFT- and TDDFT-based spectroscopic property investigations on a mixed ligand chromium(III) complex, bis [2-(2-hydroxyphenyl)benzimidazolato](1,10-phenanthroline)chromium(III) isophthalate, *Inorg. Chim. Acta* 362 (7) (2009) 2167–2171.
- A. Esparza-Ruiz, A. Pena-Hueso, R. Quijano-Quinones, A. Flores-Parra, Penta and hexacoordinated aluminum(III) compounds containing benzotriazole and benzimidazole derivatives as ligands, *Inorg. Chim. Acta* 471 (2018) 1–7.
- R.K. Dubey, U.K. Dubey, C.M. Mishra, Preparation and physico-chemical characterization of iron(III) complexes containing substituted benzimidazole and Schiff base moieties, *Transit Metal Chem* 31 (7) (2006) 849–855.
- B. Machura, M. Wolff, M. Penkala, Synthesis, X-ray studies, spectroscopic characterization and DFT calculations of $[\text{ReO}(\text{hmbzim})_2(\text{py})]\text{Cl}\cdot\text{H}_2\text{O}$ and $[\text{ReO}(\text{hpbzim})_2(\text{Hhpbzim})]\text{Cl}$, *Polyhedron* 44 (1) (2012) 156–164.
- M. Haghverdi, A. Tadjarodi, N. Bahri-Laleh, M. Nekoomanesh-Haghighi, Synthesis and characterization of Ni(II) complexes bearing of 2-(1H-benzimidazol-2-yl)-phenol derivatives as highly active catalysts for ethylene oligomerization, *Appl. Organomet. Chem.* 32 (2) (2018) 1–12.
- M. Haghverdi, A. Tadjarodi, N. Bahri-Laleh, M. Nekoomanesh-Haghighi, Cobalt complexes based on 2-(1H-benzimidazol-2-yl)-phenol derivatives: preparation, spectral studies, DFT calculations and catalytic behavior toward ethylene oligomerization, *J. Coord. Chem.* 70 (11) (2017) 1800–1814.
- Q. Shi, S. Zhang, F. Chang, P. Hao, W.-H. Sun, Nickel complexes bearing 2-(1H-benzimidazol-2-yl)-phenoxy ligands: synthesis, characterization and ethylene oligomerization, *CR Chimie* 10 (12) (2007) 1200–1208.
- I.N. Booyesen, T. Hlela, M.P. Akerman, B. Xulu, Mono- and polynuclear vanadium (IV) and (V) compounds with 2-substituted phenyl/pyridyl heterocyclic chelates, *Polyhedron* 85 (2015) 144–150.
- Y.-P. Tong, Z. Jin, Y. Chen, Synthesis, crystal structure and density functional theory study of 2-(2-hydroxyphenyl)benzimidazole based Al(III) complex co-crystallized by DMF solvate and neutral 2-(2-hydroxyphenyl)benzimidazole, *J. Chem. Crystallogr.* 41 (9) (2011) 1411–1417.
- A.K. Boudalis, J.M. Clemente-Juan, F. Dahan, V. Psycharis, C.P. Raptopoulou, B. Donnadieu, Y. Sanakis, J.-P. Tuchagues, Reversible core-interconversion of an iron(III) dihydroxo bridged complex, *Inorg. Chem.* 47 (23) (2008) 11314–11323.
- F. He, Y. Xi, J. Li, F. Zhang, Bis[2-(1H-benzimidazol-2-yl)phenolato- $\kappa^2\text{N}^3\text{O}$]cobalt(II) dimethylformamide disolvate, *Acta Crystallogr E* 64 (10) (2008) m1311.
- Y.-P. Tong, S.-L. Zheng, Synthesis, structure, spectroscopic properties, DFT and TDDFT investigations of copper(II) complex with 2-(2-hydroxyphenyl)benzimidazole, *J. Mol. Struct.* 841 (1–3) (2007) 34–40.
- A.K. Dutta, S. Samanta, S. Dutta, C.R. Lucas, L.N. Dawe, P. Biswas, B. Adhikary, Iron (III) complexes of 2-(1H-benzo[d]imidazol-2-yl)phenol and acetate or nitrate as catalysts for epoxidation of olefins with hydrogen peroxide, *J. Mol. Struct.* 1115 (2016) 207–213.
- A.K. Dutta, S.K. Maji, S. Dutta, C. Robert Lucas, B. Adhikary, Syntheses, crystal structure, spectroscopic, redox and magnetic properties of oxo- and carboxylato-bridged polynuclear iron(III) complexes with phenolate- and pyridine-substituted benzimidazole ligands, *Polyhedron* 44 (1) (2012) 34–43.
- B. Machura, M. Wolff, D. Tabak, J.A. Schachner, N.C. Moesch-Zanetti, Oxidorhenium(V) complexes with phenolate- and carboxylate-based ligands: structure and catalytic epoxidation, *Eur. J. Inorg. Chem.* (23) (2012) 3764–3773.
- A. Esparza-Ruiz, A. Pena-Hueso, I. Ramos-Garcia, A. Vasquez-Badillo, A. Flores-Parra, R. Contreras, Hypervalent triphenyl and diphenyl tin coordination compounds derived from 2-(1H-benzimidazol-2-yl)phenol, *J. Organomet. Chem.* 694 (2) (2009) 269–277.
- X. Quezada-Buendia, A. Esparza-Ruiz, A. Pena-Hueso, N. Barba-Behrens, R. Contreras, A. Flores-Parra, S. Bernes, S.E. Castillo-Blum, Synthesis and structural analyses of Co(III) coordination compounds of 2-(2'-pyridyl)benzimidazole and 2-(2-hydroxyphenyl)-1H-benzimidazole, *Inorg. Chim. Acta* 361 (9–10) (2008) 2759–2767.
- M.R. Maturya, M. Kumar, U. Kumar, Polymer-anchored vanadium(IV), molybdenum (VI) and copper(II) complexes of bidentate ligand as catalyst for the liquid phase oxidation of organic substrates, *J Mol Catal A - Chem* 273 (1–2) (2007) 133–143.
- S. Rathinasamy, S.S. Karki, S. Bhattacharya, L. Manikandan, S.G. Prabhakaran, M. Gupta, U.K. Mazumder, Synthesis and anticancer activity of certain mononuclear Ru(II) complexes, *J Enzym Inhib Med Ch* 21 (5) (2006) 501–507.
- I. Claustro, G. Abate, E. Sanchez, J.H. Acquaye, Synthesis, spectroscopic and electrochemical properties of ruthenium-2-(2'-hydroxyphenyl)benzoxazole complexes. Crystal structure of $[\text{Ru}(\text{terpy})(\text{HPB})\text{Cl}]$, *Inorg. Chim. Acta* 342 (2003) 29–36.
- G. Seth, Y. Garg, N.K. Mouraya, Studies on some biologically important ternary complexes of nickel(II) with 2-(2'-hydroxyphenyl)benzimidazole and acids, *Asian J. Chem.* 15 (1) (2003) 546–548.
- J. Cerezo, A. Requena, J. Zuniga, M.J. Piernas, M.D. Santana, J. Perez, L. Garcia, Structure, spectra, and DFT simulation of nickel benzazolate complexes with Tris(2-aminoethyl)amine ligand, *Inorg. Chem.* 56 (6) (2017) 3663–3673.
- M. Dolores Santana, R. Garcia-Bueno, G. Garcia, M.J. Piernas, J. Perez, L. Garcia, I. Lopez-Garcia, Benzazolate complexes of pentacoordinate nickel(II). Synthesis, spectroscopic study and luminescent response towards metal cations, *Polyhedron* 61 (2013) 161–171.
- M.K. Pal, N. Kushwah, D. Manna, A. Wadawale, V. Sudarsan, T.K. Ghanty, V.K. Jain, Diorganogallium and -indium complexes derived from benzoazole ligands: synthesis, characterization, photoluminescence, and computational studies, *Organometallics* 32 (1) (2013) 104–111.

- [30] L. Lopez-Banet, M.D. Santana, M.J. Piernas, G. Garcia, J. Cerezo, A. Requena, J. Zuniga, J. Perez, L. Garcia, Structure and spectroscopic properties of nickel benzazolate complexes with hydrotris(pyrazolyl)borate ligand, *Inorg. Chem.* 53 (11) (2014) 5502–5514.
- [31] M. Jiang, J. Li, Y.-q. Huo, Y. Xi, J.-f. Yan, F.-x. Zhang, Synthesis, thermoanalysis, and thermal kinetic thermogravimetric analysis of transition metal Co(II), Ni(II), Cu (II), and Zn(II) complexes with 2-(2-Hydroxyphenyl)benzimidazole (HL), *J. Chem. Eng. Data* 56 (4) (2011) 1185–1190.
- [32] M.-Y. Duan, J. Li, Y. Xi, X.-F. Lu, J.-Z. Liu, G. Mele, F.-X. Zhang, Synthesis and characterization of binuclear manganese(IV,IV) and mononuclear cobalt(II) complexes based on 2-(2-hydroxyphenyl)-1H-benzimidazole, *J. Coord. Chem.* 63 (1) (2010) 90–98.
- [33] M. Qin, D. Jin, W. Che, Y. Jiang, L. Zhang, D. Zhu, Z. Su, Fluorescence response and detection of Cu^{2+} with 2-(2-hydroxyphenyl)benzimidazole in aqueous medium, *Inorg. Chem. Commun.* 75 (2017) 25–28.
- [34] M. Sebova, V. Jorik, J. Moncol, J. Kozisek, R. Boca, Structure and magnetism of Co (II) complexes with bidentate heterocyclic ligand Hsalbim derived from benzimidazole, *Polyhedron* 30 (6) (2011) 1163–1170.
- [35] Y.-P. Tong, Y.-W. Lin, Synthesis, crystal structure and theoretical study of Al(III) complex with 2-(2-hydroxyphenyl)benzimidazole cocrystallized by DMF solvate, *Main Group Met Chem* 33 (1–2) (2010) 41–51.
- [36] Y.-P. Tong, S.-L. Zheng, X.-M. Chen, Structures, photoluminescence and theoretical studies of two Zn^{II} complexes with substituted 2-(2-hydroxyphenyl)benzimidazoles, *Eur. J. Inorg. Chem.* (18) (2005) 3734–3741.
- [37] Y.-P. Tong, Y.-W. Lin, Synthesis, crystal structure and fluorescent study of Bis(2-(2-hydroxyphenyl)benzimidazole)zinc with ethanol solvate, *J. Chem. Crystallogr.* 38 (8) (2008) 613–617.
- [38] Y.-P. Tong, S.-L. Zheng, X.-M. Chen, Syntheses, structures, photoluminescence, and theoretical studies of a class of beryllium(II) compounds of aromatic N,O-chelate ligands, *Inorg. Chem.* 44 (12) (2005) 4270–4275.
- [39] B. Machura, M. Wolff, I. Gryca, Synthesis, X-ray studies, spectroscopic characterization and DFT calculations of p-tolylmido rhenium(V) complexes bearing an imidazole-based ligand, *Polyhedron* 30 (1) (2011) 142–153.
- [40] R.K. Dubey, P. Baranwal, Synthesis, reactions and spectroscopic (UV-visible, IR, NMR (^1H - & ^{13}C)), FAB-MS, TGA and XRD) studies of new mercury(II) complexes containing various mixed ligand Schiff bases, *Main Group Met Chem* 32 (6) (2009) 321–339.
- [41] Q. Ma, M. Zhu, S. Feng, L. Lu, Bis[2-(1H-benzimidazol-2-yl)phenolato]dimethanolmanganese(III) chloride, *Acta Crystallogr E* 66 (5) (2010) m523.
- [42] H. Xu, Z.-F. Xu, Z.-Y. Yue, P.-F. Yan, B. Wang, L.-W. Jia, G.-M. Li, W.-B. Sun, J.-W. Zhang, A novel deep blue-emitting Zn^{II} complex based on carbazole-modified 2-(2-hydroxyphenyl)benzimidazole: synthesis, bright electroluminescence, and substitution effect on photoluminescent, thermal, and electrochemical properties, *J. Phys. Chem. C* 112 (39) (2008) 15517–15525.
- [43] R.K. Dubey, C.M. Mishra, Synthesis, reactions, spectral and magnetic studies of chloro(2-(o-hydroxyphenyl)benzimidazolato)cobalt(II), *Indian J Chem A* 45A (10) (2006) 2203–2208.
- [44] Y.-P. Tong, S.-L. Zheng, X.-M. Chen, Syntheses, structures, and luminescent properties of isomorphous hydroxo-bridged aluminum(III) and indium(III) compounds with 2-(2-hydroxyphenyl)benzimidazole, *Aust. J. Chem.* 59 (9) (2006) 653–656.
- [45] W. Shi, Y. Liu, B. Liu, Y. Song, Y. Xu, H. Wang, Y. Sha, G. Xu, S. Styring, P. Huang, Synthesis and characterization of a six-coordinate monomeric Mn(III) complex with SOD-like activity, *J. Coord. Chem.* 59 (2) (2006) 119–130.
- [46] M.S. Saraiva, C.I. Fernandes, T.G. Nunes, C.D. Nunes, M.J. Calhorda, New Mo(II) complexes in MCM-41 and silica: synthesis and catalysis, *J. Organomet. Chem.* 751 (2014) 443–452.
- [47] A. Tavman, A. Cinarli, D. Guerbuez, A.S. Birteksoez, Synthesis, characterization and antimicrobial activity of 2-(5-H/Me/F/Cl/NO₂-1H-benzimidazol-2-yl)-benzene-1,4-diols and some transition metal complexes, *J. Iran. Chem. Soc.* 9 (5) (2012) 815–825.
- [48] A. Tavman, S. Ikiz, A.F. Bagcigil, N.Y. Ozgur, S. Ak, Spectral characterizations and antibacterial effect of 2-(5-R-1H-benzimidazol-2-yl)-4-methyl/bromo-phenols and some metal complexes, *B Chem Soc Ethiopia* 24 (3) (2010) 391–400.
- [49] A. Tavman, S. Ikiz, A.F. Bagcigil, N.Y. Ozgur, S. Ak, Spectral characterization and antibacterial effect of 2-methyl-6-(5-H/Me/Cl/NO₂-1H-benzimidazol-2-yl)-phenols and some transition metal complexes, *Russ. J. Inorg. Chem.* 55 (2) (2010) 215–222.
- [50] A. Tavman, S. Ikiz, A.F. Bagcigil, N.Y. Ozgur, S. Ak, Synthesis, characterization, and antibacterial effect of 4-methoxy-2-(5-H/Me/Cl/NO₂-1H-benzimidazol-2-yl)-phenols and some transition metal complexes, *Turk. J. Chem.* 33 (3) (2009) 321–331.
- [51] D. Olea-Román, N. Bélanger-Desmarais, M. Flores-Álamo, C. Bazán, F. Thouin, C. Reber, S.E. Castillo-Blum, Spectroscopic studies of lanthanide complexes of varying nuclearity based on a compartmentalised ligand, *Dalton Trans.* 44 (2015) 17175–17188.
- [52] D. Olea-Roman, A. Solano-Peralta, G. Pistoris, A.L. Petrou, A. Kaloudi-Chantzzea, N. Esturau-Escofet, J. Duran-Hernandez, M.E. Sosa-Torres, S.E. Castillo-Blum, Lanthanide coordination compounds with benzimidazole-based ligands. Luminescence and EPR, *J. Mol. Struct.* 1163 (2018) 252–261.
- [53] A. Cruz-Navarro, J.M. Rivera, J. Durán-Hernández, S. Castillo-Blum, A. Flores-Parra, M. Sanchez, I. Hernández-Ahuactzi, R. Colorado-Peralta, Luminescence properties and DFT calculations of lanthanide(III) complexes ($\text{Ln} = \text{La}, \text{Nd}, \text{Sm}, \text{Eu}, \text{Gd}, \text{Tb}, \text{Dy}$) with 2,6-bis(5-methylbenzimidazol-2-yl)pyridine, *J. Mol. Struct.* 1164 (2018) 209–216.
- [54] A.G. Viveros-Andrade, R. Colorado-Peralta, M. Flores-Alamo, S.E. Castillo-Blum, J. Durán-Hernández, J.M. Rivera, Solvothermal synthesis and spectroscopic characterization of three lanthanide complexes with high luminescent properties $[\text{H}_2\text{NMe}_2]_3[\text{Ln}(\text{III})(2,6\text{-pyridinedicarboxylate})_3]$ ($\text{Ln} = \text{Sm}, \text{Eu}, \text{Tb}$): in the presence of 4,4'-Bipyridyl, *J. Mol. Struct.* 1145 (2017) 10–17.
- [55] M. Shkir, A. Abbasi, M. Faraz, A. Sherwani, Synthesis, characterization and cytotoxicity of rare earth metal ion complexes of N,N'-bis(2thiophenecarboxaldimine)-3,3'-diaminobenzidine, Schiff base ligand, *J. Mol. Struct.* 1102 (2015) 108–116.
- [56] T.F.A.F. Reji, A.J. Pearl, B.A. Rosy, Synthesis, characterization, cytotoxicity, DNA cleavage and antimicrobial activity of homodinuclear lanthanide complexes of phenylthioacetic acid, *J Rare Earth* 31 (10) (2013) 1009–1016.
- [57] C. Shiju, D. Arish, S. Kumaresan, Synthesis, characterization, cytotoxicity, DNA cleavage, and antimicrobial activity of lanthanide(III) complexes of a Schiff base ligand derived from glycylglycine and 4-nitrobenzaldehyde, *Arab. J. Chem.* 10 (2017) S2584–S2591.
- [58] A.-S. Chauvin, F. Thomas, B. Song, C.D.B. Vandevyver, J.-C.G. Bunzli, Synthesis and cell localization of self-assembled dinuclear lanthanide bioprobes, *Philos T R Soc A* 371 (1995) (2013) 1–18.
- [59] A.-S. Chauvin, S. Comby, B. Song, C.D.B. Vandevyver, J.-C.G. Bunzli, A versatile ditopic ligand system for sensitizing the luminescence of bimetallic lanthanide bioimaging probes, *Chem. Eur. J.* 14 (6) (2008) 1726–1739.
- [60] C. Saturnino, M. Bortoluzzi, M. Napoli, A. Popolo, A. Pinto, P. Longo, G. Paolucci Gino, New insights on cytotoxic activity of group 3 and lanthanide compounds: complexes with [N,N,N]-scorpionate ligands, *J. Pharm. Pharmacol.* 65 (9) (2013) 1354–1359.
- [61] Z.F. Chen, Y.Q. Gu, X.-Y. Song, Y.-C. Liu, Y. Peng, H. Liang, Synthesis, crystal structure, cytotoxicity and DNA interaction of 5,7-dichloro-8-quinolinolato-lanthanides, *Eur. J. Med. Chem.* 59 (2013) 194–202.
- [62] X. Liu, Q. Gan, C. Feng, Synthesis, characterization and antitumor activity of rare earth (Y, La) substituted phosphotungstates containing 5-fluorouracil, *J Rare Earth* 30 (6) (2012) 604–608.
- [63] G.-J. Chen, X. Qiao, C.-Y. Gao, G.J. Xu, Z.-L. Wang, J.-L. Tian, J.-Y. Xu, W. Gu, X. Liu, S.-P. Yan, Synthesis, DNA binding, photo-induced DNA cleavage and cell cytotoxicity studies of a family of light rare earth complexes, *J. Inorg. Biochem.* 109 (2012) 90–96.
- [64] G.-J. Chen, Z.-G. Wang, X. Qiao, J.-Y. Xu, J.-L. Tian, S.-P. Yan, Synthesis, DNA binding, photo-induced DNA cleavage, cytotoxicity studies of a family of heavy rare earth complexes, *J. Inorg. Biochem.* 127 (2013) 39–45.
- [65] L. Shen, Z. Lan, X. Sun, L. Shi, Q. Liu, J. Ni, Proteomic analysis of lanthanum citrate-induced apoptosis in human cervical carcinoma SiHa cells, *Biomaterials* 23 (6) (2010) 1179–1189.
- [66] H. Zhang, Y. Lan, L.-Y. Duan, E.-B. Wang, X.-L. Wang, Y.-G. Li, Z.-B. Han, Synthesis, properties and crystal structure of a new 12-molybdoorganometal salt of lanthanum coordinated to N-Methyl-2-pyrrolidone, *J. Coord. Chem.* 56 (2) (2003) 85–94.
- [67] M. Bortoluzzi, G. Paolucci, D. Fregona, L.D. Via, F. Enrichi, Group 3 and lanthanide triflate-complexes with [N,N,O]-donor ligands: synthesis, characterization, and cytotoxic activity, *J. Coord. Chem.* 65 (22) (2012) 3903–3916.
- [68] Y.-C. Liu, Z.-F. Chen, Y.-F. Shi, K.-B. Huang, B. Geng, H. Liang, Oxoglaucline-lanthanide complexes: synthesis, crystal structure and cytotoxicity, *Anticancer Res.* 34 (1B) (2014) 531–536.
- [69] C. Feng, Q. Gan, X. Liu, H. He, Hongyou synthesis and antitumor activities of rare earth substituted phosphotungstates containing 5-fluorouracil, *J Rare Earth* 30 (2012) 467–472.
- [70] X. Liu, Q. Gan, C. Feng, Synthesis, characterization and biological activity of 5-fluorouracil derivatives of rare earth (Gd, Dy, Er) substituted phosphotungstate, *Inorg. Chim. Acta* 450 (2016) 299–303.
- [71] P.S. Kuhn, L. Cremer, A. Gavriluta, K.K. Jovanovic, L. Filipovic, A.A. Hummer, G.E. Buechel, B.P. Dojcinovic, S.M. Meier, A. Rompel, Heteropentamuclear oxalato-bridged nd-4f (n = 4, 5) metal complexes with NO ligand: synthesis, crystal structures, aqueous stability and antiproliferative activity, *Chem. Eur. J.* 21 (39) (2015) 13703–13713.
- [72] D. Narayanachar, S.D. Dhumwad, V.K. Mutalik, P.V. Raj, Synthesis, spectral characterization, antimicrobial and cytotoxicity studies of some lanthanide (III) complexes of quinoline derivatives, *J. Chem. Pharm. Res.* 4 (7) (2012) 3446–3453.
- [73] L. Wang, W.-J. Li, Y.-M. Song, Antitumor activity and DNA binding studies on rare earth metal complexes with all-trans retinoic acid and L glutamic acid, *RSC Adv.* 4 (8) (2014) 42285–42292.
- [74] C. Shiju, D. Arish, S. Kumaresan, Homodinuclear lanthanide complexes of phenylthiopropionic acid: synthesis, characterization, cytotoxicity, DNA cleavage, and antimicrobial activity, *Spectrochim. Acta A* 105 (2013) 532–538.
- [75] K. Andiappan, A. Sanmugam, K. Andiappan, E. Deivanayagam, K. Karuppasamy, H.-S. Kim, D. Vikraman, In vitro cytotoxicity activity of novel Schiff base ligand-lanthanide complexes, *Sci Rep-UK* 8 (1) (2018) 3054.
- [76] T.V. Balashova, A.P. Pushkarev, V.A. Ilichev, V.A. Lopatin, M.A. Katkova, E.V. Baranov, G.K. Fukin, M.N. Bochkarev, Lanthanide phenolates with heterocyclic substituents. Synthesis, structure and luminescent properties, *Polyhedron* 50 (1) (2013) 112–120.
- [77] N.M. Lazarev, B.I. Petrov, G.A. Abakumov, M.A. Katkova, T.V. Balashova, Y.A. Bessonova, V.I. Faerman, A.V. Arapova, T.I. Lopatin, Thermochemical properties of new N,O-chelate Sc, Eu, and Tb complexes for OLED-devices, *Russ. J. Gen. Chem.* 82 (7) (2012) 1250–1253.
- [78] X. Yang, R.A. Jones, M.J. Wiestner, M.M. Oye, W.-K. Wong, Transformation of a luminescent benzimidazole-based Yb₃ cluster into a one-dimensional coordination polymer, *Cryst. Growth Des.* 10 (2) (2010) 970–976.
- [79] G. Seth, Y. Garg, Synthesis and characterisation of praseodymium (III) and neodymium (III) complexes with 2-substituted benzimidazole derivatives, *Orient. J. Chem.* 18 (2) (2002) 363–365.
- [80] M.A. Katkova, T.V. Balashova, V.A. Ilichev, A.N. Konev, N.A. Isachenkov, G.K. Fukin, S.Y. Ketkov, M.N. Bochkarev, Synthesis, structures, and

- electroluminescent properties of scandium N,O-chelated complexes toward near-white organic light-emitting diodes, *Inorg. Chem.* 49 (11) (2010) 5094–5100.
- [81] W.L.F. Armarego, C.L.L. Chai, *Purification of Laboratory Chemical*, Sixth edition, Elsevier, Inc, Butterworth-Heinemann, Burlington MA, 2009.
- [82] K.T. Papazisis, G.D. Geromichalos, K.A. Dimitriadis, A.H. Kortsaris, Optimization of the sulforhodamine B colorimetric assay, *J. Immunol. Methods* 208 (1997) 151–158.
- [83] A. Ramos-Ligonio, A. López-Monteón, A. Trigos, Trypanocidal activity of ergosterol peroxide from *Pleurotus ostreatus*, *Phytother. Res.* 26 (2012) 938–943.
- [84] GraphPad prism version 5.04 for windows, GraphPad Software, <http://www.graphpad.com>.
- [85] P.J. Hay, W.R. Wadt, *Ab initio* effective core potentials for molecular calculations – potentials for K to au including the outermost core orbitals, *J. Chem. Phys.* 82 (1985) 299–310.
- [86] W.R. Wadt, P.J. Hay, *Ab initio* effective core potentials for molecular calculations – potentials for main group elements Na to Bi, *J. Chem. Phys.* 82 (1985) 284–298.
- [87] P.J. Hay, W.R. Wadt, *Ab initio* effective core potentials for molecular calculations – potentials for the transition-metal atoms Sc to Hg, *J. Chem. Phys.* 82 (1985) 270–283.
- [88] M.J. Frisch, G.W. Trucks, H.B. Schlegel, G.E. Scuseria, M.A. Robb, J.R. Cheeseman, G. Scalmani, V. Barone, G.A. Petersson, H. Nakatsuji, X. Li, M. Caricato, A.V. Marenich, J. Bloino, B.G. Janesko, R. Gomperts, B. Mennucci, H.P. Hratchian, J.V. Ortiz, A.F. Izmaylov, J.L. Sonnenberg, D. Williams-Young, F. Ding, F. Lipparini, F. Egidi, J. Goings, B. Peng, A. Petrone, T. Henderson, D. Ranasinghe, V.G. Zakrzewski, J. Gao, N. Rega, G. Zheng, W. Liang, M. Hada, M. Ehara, K. Toyota, R. Fukuda, J. Hasegawa, M. Ishida, T. Nakajima, Y. Honda, O. Kitao, H. Nakai, T. Vreven, K. Throssell, J.A. Montgomery Jr., J.E. Peralta, F. Ogliaro, M.J. Bearpark, J.J. Heyd, E.N. Brothers, K.N. Kudin, V.N. Staroverov, T.A. Keith, R. Kobayashi, J. Normand, K. Raghavachari, A.P. Rendell, J.C. Burant, S.S. Iyengar, J. Tomasi, M. Cossi, J.M. Millam, M. Klene, C. Adamo, R. Cammi, J.W. Ochterski, R.L. Martin, K. Morokuma, O. Farkas, J.B. Foresman, D.J. Fox, Gaussian 16, Revision B.01, Gaussian, Inc., Wallingford CT, 2016.
- [89] M.K. Assefa, J.L. Devera, A.D. Brathwaite, J.D. Mosley, M.A. Duncan, Vibrational scaling factors for transition metal carbonyls, *Chem. Phys. Lett.* 640 (2015) 175–179.
- [90] M.V. Castillo, E. Romano, H.E. Lanús, S.B. Dfáz, A. Ben Altabef, S.A. Brandán, Theoretical structural and experimental vibrational study of niobyl nitrate, *J. Mol. Struct.* 994 (1–3) (2011) 202–208.
- [91] ChemCraft, Graphical Software for Visualization of Quantum Chemistry Computations, <http://www.chemcraftprog.com>.
- [92] Diamond, Crystal and Molecular Structure Visualization, <http://www.crystalimpact.com/diamond>.
- [93] K. Nakamoto, Applications in coordination chemistry, *Infrared and Raman Spectra of Inorganic and Coordination Compounds: Part B: Applications in Coordination, Organometallic, and Bioinorganic Chemistry*, Sixth edition, John Wiley & Sons, Inc, Hoboken, NJ, USA, 2008.
- [94] K. Nesmerak, Lanthanide/actinide in health and disease, in: R.H. Kretsinger, V.N. Uversky, E.A. Permyakov (Eds.), *Encyclopedia of Metalloproteins*, Springer, New York, NY, 2013.